Design of the Advanced LIGO recycling cavities

Muzammil A. Arain* and Guido Mueller
Department of Physics, University of Florida, Gainesville, FL, 32611-8440
muzamil@phys.ufl.edu

Abstract: The current LIGO detectors will undergo an upgrade which is expected to improve their sensitivity and bandwidth significantly. These advanced gravitational-wave detectors will employ stable recycling cavities to better confine their spatial eigenmodes instead of the currently installed marginally stable power recycling cavity. In this letter we describe the general layout of the recycling cavities and give specific values for a first possible design. We also address the issue of mode mismatch due to manufacturing tolerance of optical elements and present a passive compensation scheme based upon optimizing the distances between optical elements.

OCIS codes: (120) Instrumentation, measurement, and metrology; (120.2230) Fabry-Perot;(120.3180) Interferometry; (350.4600) Optical Engineering.

References and links

1. S. J. Waldman et. al., "Status of LIGO at the start of the fifth science run," Class. Quantum Grav. **23,** S267–S269 (1999).
2. R. Adhikari, P. Fritschel, and S. Waldman, "Enhanced LIGO," LIGO document, LIGO-T060156-01, http://www.ligo.caltech.edu/docs/T/T060156-01.pdf.
3. A. Weinstein, "Advanced LIGO optical configuration and prototyping effort," Class. Quantum Grav. **19,** 1575–1584 (2002).
4. C. Wilkinson, "Plans for Advanced LIGO Instruments," presented at the 2005 APS April Meeting, Tampa, Florida, USA, 16-19 April 2005.
5. A. M. Gretarsson, E. D'Ambrosio, V. Frolov, B. O'Reilly, and P. K. Fritschel, "Effects of mode degeneracy in the LIGO Livingston Observatory recycling cavity," J. Opt. Soc. Am. B **24,** 2821–2828 (1999).
6. S. Ballmer et al., "Thermal Compensation System Description," LIGO document, LIGO- T050064-00-R, http://www.ligo.caltech.edu/docs/T/T050064-00.pdf.
7. H. Armandula et al., "Core Optics Components Preliminary Design," LIGO document LIGO- E080033-00-D , http://www.ligo.caltech.edu/ gari/LIGOII/E080033-00PreliminaryDesign.pdf.
8. H. Armandula et al., "Core Optics Components Preliminary Design," LIGO document LIGO- E080033-00-D , http://www.ligo.caltech.edu/ gari/LIGOII/E080033-00PreliminaryDesign.pdf.
9. P. Fritschel, "Second generation instruments for the Laser Interferometer Gravitational Wave Observatory (LIGO)," Proc. SPIE **4856,** 282–291 (2003).
10. H. Yamamoto, "Scattering Loss," presented at the LIGO-Virgo meeting, Hannover, Germany, October 2007, www.ligo.caltech.edu/docs/G/G070657.pdf.
11. D.A. Shaddock et al., "Power-recycled Michelson interferometer with resonant sideband extraction," Appl. Opt. **42,** 1283–1295 (2003).
12. M. A. Arain et al., "Input Optics Subsystem Preliminary Design Document," LIGO document, LIGO-T060269-02-D, http://www.ligo.caltech.edu/docs/T/T060269-02.pdf.
13. Y. Pan, "Optimal degeneracy for the signal-recycling cavity in advanced LIGO," http://arxiv.org/PS_cache/gr-qc/pdf/0608/0608128v1.pdf.
14. G. Mueller, "Stable Recycling Cavities for Advanced LIGO," LIGO document LIGO-G050423-00-Z, http://www.ligo.caltech.edu/docs/G/G050423-00/G050423-00.pdf.
15. M. A. Arain, "Thermal Compensation in Stable Recycling Cavity," presented at the LSC March meeting, Louisiana, USA, March 2006, http://www.ligo.caltech.edu/docs/G/G060155-00/G060155-00.pdf.

#96414 - $15.00 USD Received 19 May 2008; revised 17 Jun 2008; accepted 17 Jun 2008; published 23 Jun 2008

16. G. Mueller, "Stable recycling cavities for Advanced LIGO," presented at the LIGO-Virgo meeting, Hannover, Germany, October 2007, available at www.ligo.caltech.edu/docs/G/G070691-00.pdf.
17. G. Heinzel et al, "Dual recycling for GEO 600," Class. Quantum Grav. **19,** 1547–1553 (2002).
18. G. Heinzel et al, "Experimental Demonstration of a Suspended Dual Recycling Interferometer for Gravitational Wave Detection," Phys. Rev. Lett. **81,** 5493–5496 (1998).
19. F Acernese et al, "Status of Virgo," Class. Quantum Grav. **22,** S869–S880 (2002).
20. R. Takahashi et al., "Status of TAMA300," Class. Quantum Grav. **22,** S403–S408 (2004).
21. G. Mueller, "Parametric Instabilities and the geometry of the recycling cavities," presented at the Parametric Instability Workshop, Perth, Australia, 16-18 July, 2007, www.ligo.caltech.edu/docs/G/G070441-00.pdf.
22. N. Mavalvala, D. Sigg, and D. Shoemaker, "Experimental Test of an Alignment-Sensing Scheme for a Gravitational-Wave Interferometer," Appl. Opt. **37,** 7743–7746 (2005).
23. G. Mueller, "Beam jitter coupling in advanced LIGO," Opt. Express **13,** 7118–7132 (2005), http://www.opticsinfobase.org/abstract.cfm?URI=oe-13-18-7118.
24. E. Siegman, *Lasers* (University Science Books 1986).
25. R. Lawrence, "Active Wavefront Correction in Laser Interferometric Gravitational Wave Detectors," PhD Dissertation, Massachusetts Institute of Technology, (2003).

1. Introduction

The direct observation of Gravitational waves (GW) has been the elusive goal of several ambitious projects worldwide. The most sensitive observatories today are the NSF funded Laser Interferometer Gravitational Wave Observatories (LIGO) in Hanford, WA, and Livingston, LA. These observatories consist of 4 km long highly optimized Michelson interferometer which reach displacement sensitivities below $10^{-18}\mathrm{m}/\sqrt{\mathrm{Hz}}$ between 70 and 1000 Hz. LIGO just finished its fifth science run [1] and the LIGO Science Collaboration (LSC) is currently analyzing the data while the detectors are being upgraded. This upgrade is known as enhanced LIGO. The main changes are an increase in the laser power, improved input optics components to handle this laser power, the installation of additional optical baffles to reduce stray light, and the addition of DC sensing. These changes will improve the sensitivity by an additional factor of two to three depending on the frequency of interest. It is expected that this upgrade will be completed in the fall of 2008 and will be followed by a new year-long science run [2].

This is followed by another major upgrade called Advanced LIGO. This upgrade includes a further increase in the laser power, and major changes in the optical configuration, in the suspension systems, and in virtually all other relevant subsystems [3, 4]. Advanced LIGO will open up the sub-50 Hz frequency range and will also improve the peak sensitivity above 50 Hz significantly. One change is the addition of signal recycling which allows to tune the frequency dependent sensitivity curve by changing the length of the signal recycling cavity (SRC).

In this paper we discuss the design constraints, tolerances, and the current design of the power recycling cavity (PRC) and SRC in Advanced LIGO. Their design will be substantially different from the design of the PRCs employed in the current LIGO interferometer.

2. LIGO Configuration

Each of the current LIGO interferometer starts with a 10 W laser system. The laser beam is then handed over to the input optics where it's phase is modulated with 24.5 MHz and 33 MHz by a series of electro-optical modulators (EOM). The spatial mode is cleaned with a suspended triangular mode cleaner before it is send through a Faraday isolator and a beam expanding telescope into the main interferometer. Figure 1 shows the central part of the main LIGO interferometer. It is a Michelson interferometer with 4 km long identical Fabry Perot cavities in each arm. The cavity input mirrors (ITMs) have a transmission of $T_I = 2.7\%$ and a radius of curvature (ROC) R_{ITM} of about 15 km and the end mirrors (ETMs) have a transmission of about $5-10$ ppm and a ROC R_{ETM} of about 7 km. Consequently, each arm cavity is highly over-coupled and on resonance the reflected field will be dominated by the field leaking out of the cavity. This changes

#96414 - $15.00 USD Received 19 May 2008; revised 17 Jun 2008; accepted 17 Jun 2008; published 23 Jun 2008

the phase of the reflected field by 180° compared to the case where the arm cavity would be non-resonant. Each Fabry Perot cavity resonates on the same fundamental Gaussian mode. This mode has a beam radius at the ITM of 3.7 cm and a Rayleigh range of 4000 m inside the arm cavities and of 3700 m inside the short Michelson interferometer. These modes (red) interfere again at the beamsplitter such that virtually all the light is sent back towards the Faraday rotator.

A small asymmetry in the distances between the beamsplitter and the ITMs allows the 24.5 MHz modulation sidebands (blue) to reach the dark port. GW will modulate the length of each arm cavity and generate sidebands (green) around the carrier which are offset from the carrier frequency by the GW frequency. Because of the quadrupole nature of the GW, these signal sidebands will interfere at the beamsplitter in such a way that they are transmitted to the dark port. There they beat against the 24.5 MHz sidebands to generate the main science signal. The efficiency of the beat signal between the signal sidebands and the RF sidebands depends on the modal overlap between both fields.

An additional mirror is placed between the beam expanding telescope and the beamsplitter. This power recycling mirror (PRM) forms the input mirror of the PRC. The 'end mirror' of this cavity is the Michelson interferometer. The PRM has a transmissivity of $T_{PR} = 2.7\%$ and increases the circulating power by about 50. This transmissivity was chosen based on the expected losses for the carrier field which resonates in the arm cavities. The goal was to create a slightly over-coupled PRC for the carrier field.

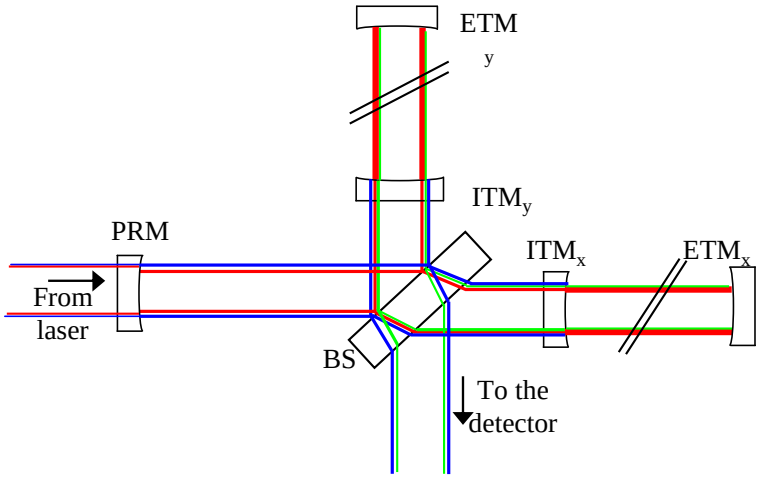

Fig. 1. The current LIGO configuration uses two 4 km long arm cavities formed between the ITMs and ETMs in each arm of a Michelson interferometer. The PRM and the Michelson interferometer form the PRC. The carrier (red) resonates inside the arm cavities and the PRC, the RF-sdiebands (blue) resonate inside the PRC, and the signal sidebands (green) resonate inside the arm cavities and propagate to the detector in the dark port. The different 'beam sizes' symbolize the different spatial modes of the various fields in the various cavities.

The 24.5 MHz sidebands are only resonating between the PRM and the short Michelson interferometer before they reach the dark port. This PRC has a length of about 9.2 m. This is much shorter than the Rayleigh range of the Gaussian eigenmode which is expected to propagate in this cavity. Furthermore, the entire cavity is located in the far field of the eigenmode. Therefore the transversal mode spacing of the PRC is only about 11 kHz which is well below the 350 KHz linewidth of the recycling cavity. Such a cavity is only marginally stable and any small distortion will lead to resonantly enhanced scatter between the spatial modes and can

#96414 - $15.00 USD Received 19 May 2008; revised 17 Jun 2008; accepted 17 Jun 2008; published 23 Jun 2008

push the cavity easily into a region where it is unstable. However, as the fundamental mode of the carrier field inside the recycling cavity experiences a 180° phase shift at the arm cavities all higher order modes of the carrier are virtually anti-resonant inside the PRC. This leads to a very stable spatial eigenmode for the carrier field inside the otherwise only marginally stable PRC. The RF sidebands never reach the inside of the arm cavities and their spatial mode is not filtered by them. Many higher order modes of the RF sidebands are resonant and build up as soon as they are excited by mode mismatch, angular motions of the mirrors, or simply scatter between the modes [5]. This leads to substantial spatial mode mismatches between the carrier, the RF-sidebands, and the signal sidebands. Only the installation of a sophisticated thermal compensation system allowed to reach the current sensitivity of LIGO[6].

3. Advanced LIGO

Several differences between LIGO and Advanced LIGO will aggravate the problem of unstable recycling cavities. First, the beam sizes on the test masses increase to reduce thermo-elastic noise caused by the Brownian motion of the atoms on the surfaces of the mirrors. The current design carries radii of curvatures for the ITMs of 1971 m and for the ETMs of 2191 m. This leads to beamsizes of $w_{ITM} = 5.55$ cm ($1/e^2$ intensity beam radius) on the ITMs and of $w_{ETM} = 6.2$ cm on the ETMs [7, 8]. Note that this has changed from the original symmetric design of $R_{ITM} = R_{ETM} = 2076$ m and beamsizes of 6 cm to reduce diffraction losses inside the recycling cavities and to take into account the scaling of the thermo-elastic noise with the number of coating layers [9, 10].

In addition to power recycling, Advanced LIGO will also employ signal recycling. The signal sidebands will be sent back into the interferometer where they can be coherently enhanced or used to coherently extract more sideband amplitude from the arm cavities. In the later case, the SRM is placed at a position where the carrier is resonant in the SRC which increases the effective transmissivity of the ITMs. The subsequent reduction in the finesse increases the bandwidth of the entire detector. This is called resonant sideband extraction [11]. Changing the position of the SRM will increase the peak displacement sensitivity in a position dependent specific frequency range but will also reduce the bandwidth of the detector. This is commonly known as detuned signal recycling or detuned resonant sideband extraction.

In the original baseline design of Advanced LIGO the SRC was also a marginally stable cavity designed very much like the PRC [12]. The PRC in combination with the arm cavities is resonant for the carrier. In contrast the SRC in combination with the arm cavities is anti-resonant. This would make the higher order spatial modes of the signal sidebands to be resonant or near resonant in the SRC unless these sidebands gain a significant Gouy phase. Similar to the RF sidebands in the current PRC, any ROC mismatches or angular motions of the mirrors would have led to resonantly enhanced mode scatter and reduced gravitational wave signals [13]. Although a thermal compensation system will also be employed in Advanced LIGO to correct ROC mismatches, the requirements on this system would have increased significantly due to the increased laser power and subsequent thermal lensing, the increased beam diameters on the ITMs which would have driven these marginally stable recycling cavities even closer to the unstable region, and the improved sensitivity which puts stringent requirements on the technical noise in the thermal compensation system. This was realized already a few years ago and a new design for the recycling cavities was discussed and finally adopted for Advanced LIGO in the beginning of this year [14-16].

It should be noted that signal recycling has been tested at the GEO detector [17]; GEO does not use arm cavities, various table top experiments [18] with and without arm cavities, and is currently being tested again at the 40m prototype at the California Institute of Technology with arm cavities. All these test interferometers employed or employ stable recycling cavities while

#96414 - $15.00 USD Received 19 May 2008; revised 17 Jun 2008; accepted 17 Jun 2008; published 23 Jun 2008

LIGO, VIRGO, and TAMA are using marginally stable power recycling cavities [19, 20] and no signal recycling.

The new recycling cavity design uses three mirrors instead of one for each recycling cavity (see Figure 2); a two mirror design which is also possible but has severe practical problems will be discussed in the Appendix. The distances between the three mirrors are restricted by the locations of the horizontal access modules (HAM) which are essentially suspended optical tables inside the LIGO vacuum system. The mirrors have to be suspended and have to share the HAM tables with other optical components such as the suspended mirrors of the input mode cleaner (MC), the in-vacuum Faraday isolator, and multiple steering mirrors. Possible distances are in the order of 15 to 16 m to give the reader an idea of the scales involved.

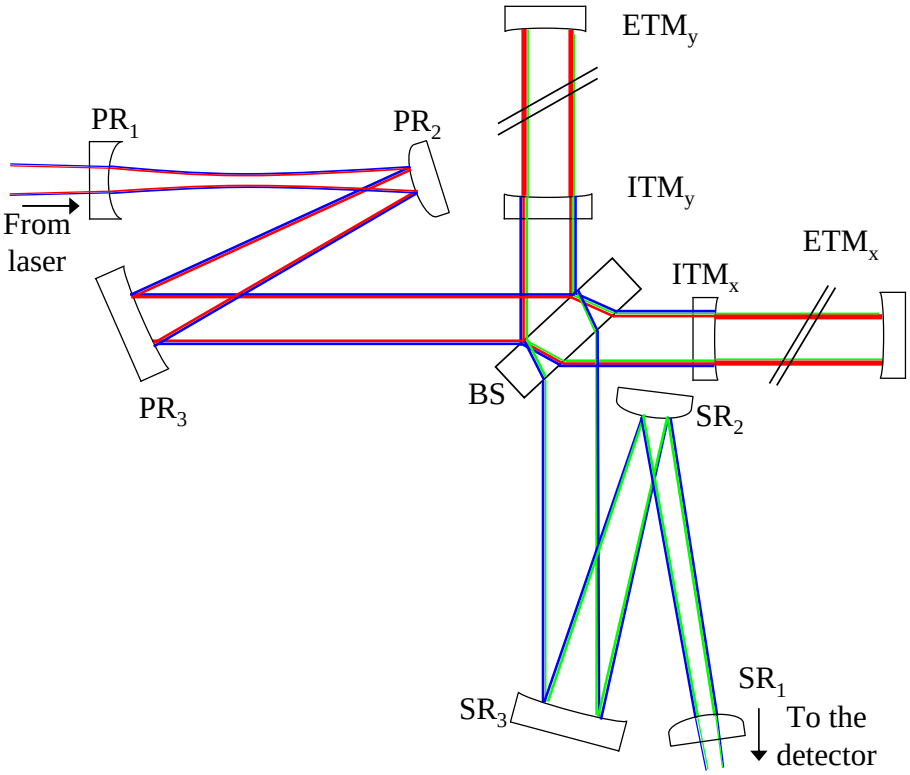

Fig. 2. The Advanced LIGO design uses three mirror recycling cavities. Each recycling cavity consists of a beam expanding (or reducing) telescope (PR_3/PR_2 or SR_3/SR_2, respectively) and an additional end mirror PR_1 or SR_1. The position of the end mirror with respect to the waist of the mode going to PR_2 or coming from SR_2 determines the final Gouy phase inside each recycling cavity. The red lines indicate the carrier eigenmode, the blue lines the eigenmode of the RF sidebands, and the green line of the signal sidebands. After optimizing the beam expanding and reducing telescopes all spatial modes will be well matched to each other.

Before presenting the current set of specific values for ROCs and mirror locations, we discuss general aspects of both stable recycling cavities. These general aspects will not change while the specific values are still being optimized to ensure for example that all optical components

#96414 - $15.00 USD Received 19 May 2008; revised 17 Jun 2008; accepted 17 Jun 2008; published 23 Jun 2008

fit inside the vacuum envelope without blocking parts of the various laser beams. It should also be noted that the overall length of each recycling cavity is set by the RF sidebands which have to resonate in these cavities to generate the necessary length and angular control signals. This puts additional constrains on the design.

The spatial mode coming from the ITM will be focused by the large R_3 (PR_3 or SR_3) mirror. The convergence angle between R_3 and R_2 (PR_2 or SR_2) will be in the order of a few mrad (see also Appendix). This highly converging beam propagates over a distance of about 16 m to R_2 . Before this mode reaches its own Rayleigh range, R_2 reduces the convergence angle and sends the light to R_1 (PR_1 or SR_1). As R_2 changes the modal parameters before the mode reaches its own Rayleigh range, the accumulated Gouy phase between the mirrors R_2 and R_3 is very small. The location of the waist of the mode between R_1 and R_2 with respect to the location of R_1 is responsible for the accumulated Gouy phase and consequently for the transversal mode spacing and the stability of the recycling cavities. This location depends on the ROC of R_2 . Figure 3 shows the accumulated Gouy phase and the beam size on R_1 as a function of the ROC of R_2 for a typical fixed distance between R_2 and R_1 and a typical ROC of R_3 .

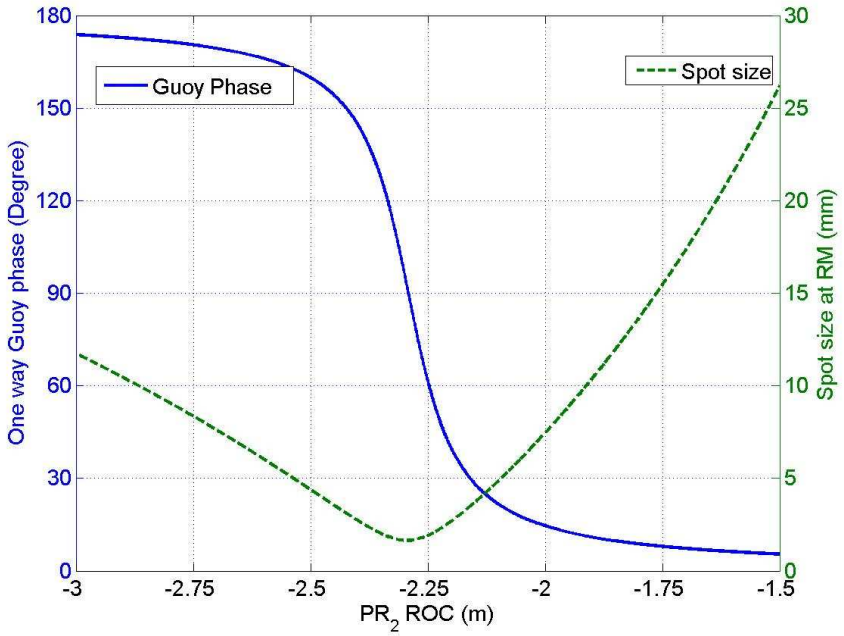

Fig. 3. The accumulated Gouy phase (blue, left axis) and the beam size (green, right axis) on R_1 as a function of the ROC of R_2 . The minimum spot size is 1.6 mm at a Gouy phase of 90°.

The accumulated Gouy phase will still be small if the Rayleigh range of this mode is smaller than the distance between the waist location and R_1. But by decreasing the (negative) ROC of R_2, the waist location can be pushed closer and closer to R_1. Once the distance between the waist and R_1 is smaller than the Rayleigh range, the mode will start to accumulate Gouy phase inside the SRC and the transversal mode spacing will become larger than the linewidth of the recycling cavity. Our current design of the SRC is similar to this case and the one-way Gouy phase in the SRC is currently set to $\Psi_G^{SR} = 0.51$ rad. For the PRC, we further decrease the ROC of PR_2 and move the waist into the PRC. Once the waist is inside the cavity, the Gouy phase is

#96414 - $15.00 USD Received 19 May 2008; revised 17 Jun 2008; accepted 17 Jun 2008; published 23 Jun 2008

larger than $\pi/2$. Our current design of the power recycling cavity is similar to this case and the one-way Gouy phase in the PRC is currently set to $\Psi_G^{PR} = 2.08\,\mathrm{rad}$.

These specific Gouy phases were chosen such that the lowest order transversal modes other than the fundamental mode are at least one full linewidth away from resonance inside any of the recycling cavities [21]. This includes the transversal modes of the carrier, the signal sidebands, and the RF sidebands. The above values fullfil this condition for a transmissivity of the signal recycling mirror of $T_{SR} \approx 7\%$ when the SRC is resonant for the carrier (resonant sideband extraction). However, it has to be realized that it is impossible to fullfil this condition for all possible tunings of the signal recycling cavity. Additional optimization will require identification of a certain (hopefully small) number of potential tunings for the SRC and then optimization of the Gouy phases for these specific points of operation. Note that the difference between the Gouy phases $\Psi_G^{PR} - \Psi_G^{SR} = \pi/2$causes degeneracy in the transversal mode spectrum which reduces the problem to some degree. This specific difference has another advantage as long as the SRC is tuned on or near the resonant sideband extraction tuning. The Michelson interferometer formed by the two recycling cavities reflects all odd modes and transmits all even modes generated in one of the arms. Although the visibility is not perfect because the reflectivities of the two recycling cavity mirrors are not equal, the amplitude of an odd mode will be much higher in the arm where it is generated compared to the other arm where it is not generated. The odd modes include the (1,0) and (0,1) Hermite Gauss modes which are generated by alignment errors of the mirrors. The amplitudes of these modes are measured at various ports to generate alignment signals for all optical components. With this specific Gouy phase difference it is possible to differentiate between alignment errors in the X and the Y-arm of the main interferometer by using spurious reflections in each arm to generate the alignment sensing signals. The signals in the X-arm are fairly independent from any misalignments in the Y-arm and vice versa. This choice of Gouy phases also allows to track modes which are generated for example by parametric instabilities better which could help during commissioning to identify their source and to suppress them.

The current design parameters as well as the beam sizes and the accumulated one-way Gouy phases for the stable recycling cavities are shown in Table 1. These design parameters are calculated using ABCD matrices and Gaussian modes to describe and propagate the laser field inside the interferometer. Note that the final design parameters are likely to be slightly different from these parameters as the final layout is currently revisited to include changes in the length and alignment sensing system and to fit all components into the vacuum system without clipping the various laser beams. However, the results presented in the remainder of this paper will not change significantly.

Table 1. The current design parameters for the stable PRC and the stable signal recycling cavity. R_i are the radii of curvature of the three mirrors PR_i or SR_i. L_{ij} are the distances between mirrors ij; Index I stands for the ITM mirror. The one-way Gouy phases in the recycling cavities are: $\Psi_G^{PR} = 2.08\,\mathrm{rad}$, $\Psi_G^{SR} = 0.51\,\mathrm{rad}$.

	PR_1	PR_2	PR_3	SR_1	SR_2	SR_3
Radius [m]	8.220	-2.346	34.750	-15.373	-3.261	34.000
Beamsize [mm]	1.75	3.45	56.52	2.22	5.03	56.50
	L_{12}	L_{23}	L_{3I}	L_{12}	L_{23}	L_{3I}
Distance [m]	15.760	16.523	25.394	15.421	15.680	24.928
Gouy Phase [rad]	2.054	0.029	0.003	0.488	0.019	0.003

#96414 - $15.00 USD Received 19 May 2008; revised 17 Jun 2008; accepted 17 Jun 2008; published 23 Jun 2008

4. Requirements on Mode matching

LIGO and also Advanced LIGO depend strongly on beat signals between the carrier field, the RF-sidebands, and the signal sidebands. These beat signals are taken at various locations and are used to extract the GW information, control all longitudinal and alignment degrees of freedom, and potentially even measure the mode mismatches between the various fields [22, 23]. The amplitudes of the beat signals scale with the spatial overlap between the transversal modes of each of these frequency components. Any mismatch between the spatial modes will reduce each of these signals. In addition, the higher order modes in each frequency component will beat against higher order modes in other frequency components and will generate spurious signals. Therefore it is important to calculate the coupling between the resonating modes of the various cavities.

In this paper the eigenmode of each cavity is calculated using the complex q-parameters and the standard matrix formalism. When

$$M = \begin{pmatrix} A & B \\ C & D \end{pmatrix}$$

describes a roundtrip in the cavity, the complex q-parameter of the cavity eigenmodes has to be a solution of the following equation [24]:

$$q = \frac{Aq+B}{Cq+D}$$

In this formalism we do not take into account the coupling between the cavities which changes the spatial eigenmode in each cavity. This change depends on the type and magnitude of the mismatch, the coupling coefficients, and also the resonance condition of the coupled cavities. A quantitative analysis of these effects is beyond the aim of this paper but some quantitative results for the SRC can be found in [5].

4.1. Signal recycling cavity

Advanced LIGO will employ DC-sensing instead of RF-sensing. In this sensing scheme the main signal in Advanced LIGO will be the beat signal between the signal sidebands and the carrier at the dark port. Mode mismatches between the SRC and the arm cavities will reduce the build-up of the signal sidebands in the SRC and will reduce the modal overlap with the leakage field of the carrier. Any compensation of this signal loss by increasing the laser power would automatically increase the carrier build-up inside the arm cavities. The increased radiation pressure noise would deteriorate the low frequency sensitivity. Consequently, a performance independent compensation of these losses is impossible.

The GW signal strongly depends upon the mode matching between the carrier signal and the signal sideband in the SRC. A 0.1% drop in mode matching decreases the GW signal by as much as 5% [13]. Various effects including imperfactions in TCS, scattering, wedge angle at BS, and diffraction effects at BS may contrubute to this loss. We can use that loss mechanism to impose an upper limit of 0.1% allowable mode mismatch between the recycling cavity and the arm cavity mode.

4.2. Power recycling cavity

As the RF sidebands are not resonant in the arm cavities, their eigenmode is completely determined by the ROC of the mirrors forming the PRC. In contrast to this, the eigenmode of the carrier is dominated by the arm cavity eigenmode. Any mismatch between the two eigenmodes will reduce the build-up of the carrier inside the arm cavities as the carrier has to propagate

#96414 - $15.00 USD Received 19 May 2008; revised 17 Jun 2008; accepted 17 Jun 2008; published 23 Jun 2008

through the PRC and will reduce the spatial overlap between the carrier and the RF sidebands. The reduction in the carrier build-up can in principle be compensated by increasing the laser power. This increase is possible until the maximum laser power is reached or until the photo detector which senses the reflected field saturates. An increase of the laser power will also increase the amount of scattered light which has become one of the main problems in all interferometric GW detectors. However, the main problem of the modal mismatch between the PRC and the arm cavities is that it will create a difference between the spatial modes of the RF sidebands and the spatial mode of the carrier. This mismatch deteriorates all beat signals used for length and alignment sensing and control.

Although the effect of the modal mismatch in PRC has not been modeled in detail, the requirements are less stringent than the SRC.

4.3. General properties of both designs

As discussed in the last paragraphs, the Gouy phase is mainly a function of the ROC of the second mirror, i.e, PR_2 or SR_2 and of the distance between the first and the second mirror. The mode matching between each recycling cavity and the arm cavities can be changed by changing the distances between the three mirrors and also the distance to the arm cavity. However, the change scales in general with the Rayleigh range of the Gaussmode which is received or send out by the mirror that is repositioned. The Rayleigh range in the part between the ITM and R_3 will be around 200 m in Advanced LIGO. Any substantial change in mode matching in this part would require to move the mirrors with respect to each other by several 10 m. This is impossible given the vacuum contraints in LIGO. On the other hand, this also means that even changes in the distance of up to a few meter will not affect the mode matching. The Rayleigh range in the part between R_2 and R_1 is on the order of a few meters (≈ 4.1 m in the power recycling cavity and ≈ 7.7 m in the signal recycling cavity). Any substantial change in the mode matching in this part would also require to move the mirrors by at least several 10 cm. Although possible, this would still require major additional changes as the overall length of the recycling cavities has to be preserved to ensure that the RF-sidebands are resonant in the recycling cavities.

The mode matching is only sensitive to the beam expanding telescopes which are formed between R_2 and R_3 . The Rayleigh range of the mode propagating between these two mirrors is only ≈ 3.3 cm in the PRC and ≈ 3.1 cm in the SRC. Consequently, any change in the ROCs or distances on scales of a few cm will change the mode matching significantly. The fact that the mode matching is rather insensitive to the other distances allows us to optimize the mode matching without changing the overall lengths of the recycling cavities. Any change in the distance between R_2 and R_3 will simply be compensated by also changing the distance between R_2 and R_1 by twice that much; changing the distance between R_3 and the ITMs would be even better from a mode matching point of view but R_3 is a much larger mirror and would require much more available real estate for this move than the smaller R_1 mirror.

This strong sensitivity to the distance between R_2 and R_3 can also be understood in terms of ray optics. The field coming from R_2 appears to orginate from a virtual point source behind R_2. The distance between this virtual source is roughly half of the ROC of R_2 . R_3 is then placed close to half of its ROC away from the virtual focus and creates an image of the focus several km away. A small change of δR_2 in the ROC of R_2 will change the location of the virtual point source by about $\delta R_2/2$. A change of δR_3 in the ROC of R_3 will change where the location of the virtual source should be to focus the beam to the right spot by $\delta R_3/2$. As the image of the focus is several km away, a small change in any of the two radii curvatures in the wrong direction pushes the image even further out leading to an unstable mode inside the recycling cavities. However, both changes or deviations in the radii of curvatures can be compensated by changing the distance between R_2 and R_3 by $\delta L_{23} \approx \delta R_3/2 + \delta R_2/2$ creating

#96414 - $15.00 USD Received 19 May 2008; revised 17 Jun 2008; accepted 17 Jun 2008; published 23 Jun 2008

again a very stable recycling cavity. Although this will also affect the beamsizes and reduce the mode matching again, the change in beamsizes are rather small and, as we will see in the following chapter, will not reduce the modematching significantly.

5. Tolerances on the radii of curvatures

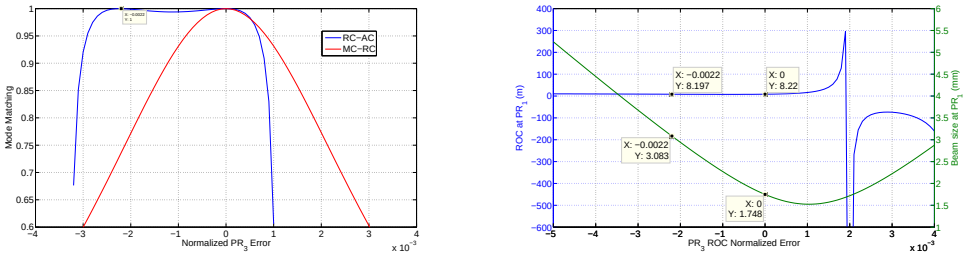

Fig. 4. Left graph: The blue line shows the mode matching (in power) between the PRC and the arm cavity eigenmode as a function of the normalized error in PR_3 ROC. The red line shows the mode matching between the input field coming from the mode cleaner and the recycling cavity. Right graph: The ROC plotted on left y-axis and beam size plotted on right y-axis. For two different values of PR_3 ROC, we have the same ROC (and hence a stable solution) at PR_1 with 100% mode matching. The modematching as a function of the ROC of PR_2 behaves similar in terms of absolute error in ROC. The signal recycling cavity shows also the same behavior. Here AC: Arm cavity, RC: Recycling cavity, and MC: Mode cleaner.

Advanced LIGO has to take into account manufacturing tolerances in ROCs of all interferometer mirrors. The design of the interferometer should either be sufficiently insensitive to ROC mismatches or be flexible to compensate for them. In initial LIGO, the thermal compensation system attempts to match the marginally stable PRC to the arm cavities while at the same time maintaining a good visibility of the Michelson interferometer. A similar system will also be used in Advanced LIGO but its main goal will be to improve the visibility of the Michelson interferometer by matching the two spatial modes coming from the arms and to compensate for any thermal lensing that occurs especially in the ITM substrates [25]. Consequently, the requirements on the mode matching derived in the last section translates directly into requirements on ROCs of the various mirrors or on our ability to adjust the mode matching.

5.1. ROC Tolerance of PRC and SRC

The recycling mirrors PR_2 (SR_2) and R_3 (SR_3) form relatively fast telescopes inside the recycling cavities. Consequently, the spatial eigenmode inside the recycling cavities is very sensitive to any ROC error in these mirrors. Comparatively, the remaining mirror, i.e., PR_1 (SR_1) has much relaxed ROC error tolerances. For simplicity, we will discuss PRC in the remainig of the section as the behavior of SRC is very silimar. The blue curve in the left graph in Figure 4 shows the mode matching between the recycling cavity eigenmode and the arm cavity eigenmode as a function of the error in PR_3 ROC. It shows two maxima where the modematching is 100%. The reason for the two maxima lies in the dependence of the ROC of a Gaussmode from the distance to its waist:

$$R = z + \frac{z_R^2}{z}.$$

#96414 - $15.00 USD Received 19 May 2008; revised 17 Jun 2008; accepted 17 Jun 2008; published 23 Jun 2008

This function has a minima at $z = z_R$. A change in the ROC of PR_3 will move the waist further away from PR_1. During the change the ROC of the mode at PR_1 will run through the minima and increase again. Consequently, it will match twice to the ROC of the PR_1 mirror. The first solution corresponds to the design Gouy phase of 2.08rad while the second solution has a one-way Gouy phase of π-2.08=1.06rad. Although the ROCs match, the beam sizes are quite different for these two solutions. Therefore, the mode matching from the MC is only good for first solution. Changes in the ROC of PR_2 shows a similar behavior but as the ROC is smaller the normalized error tolerance is larger. The SRC shows essentially the same behavior.

An increase of the ROC of PR_3 of only 0.1% destabilizes the spatial eigenmodes of the recycling cavities. However, adjusting the distance between PR_2 and PR_3 while maintaining the recycling cavity length by moving PR_1 by twice the distance allows to regain the stable recycling cavity modes and improve the mode matching back to 99.998% for deviations up to ± 15 cm in the recycling cavity mirrors ROCs. Figure 5 shows the mode matching sensitivity to the position of PR_2. The blue curve shows the mode matching as a function of PR_2 position from its nominal position when PR_2 and PR_3 are at their nominal ROC values. The curve has two maximums, i.e, one at the nominal position and the other 40 mm from its nominal position. The reason for the two maxima is again the hyperbolic behaviour of the ROC of the phasefront as a function of the distance to the waist. The same behavior can be observed even when the ROCs of PR_2 and PR_3 differ from their nominal values as shown by the green curve. The red and golden curves show the product of mode matching between MC to recycling cvaity and recycling cavity to arm cavityas a function of the position of PR_2. Again, only one of the maxima in the mode matching between the recycling cavity and the arm cavity eigenmodes coincides with a good modematching of the input beam. In any case, as the Fig. 5 suggests the expected polishing error in ROCs of PR_2 and PR_3 can be corrected by appropriately repositioning the PR_2 and PR_1 mirror.

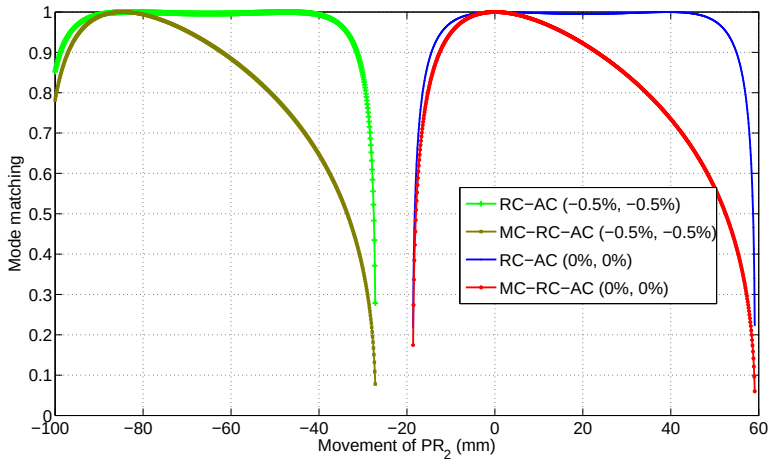

Fig. 5. The mode matching (in power) as a function of displacement of R_2 (it applies to both PR_2 and SR_2) from the nominal position. The blue curve shows the mode matching between the recycling cavity and the arm cavity for nominal ROC values of PR_2 and PR_3 while the green curve is for -0.5 percent error in the nominal ROC values of PR_2 and PR_3. The red and the golden curves show the corresponding mode matching product from the input (or output) mode cleaner mode to the PRC (SRC) mode and then from PRC to the arm cavity mode for nominal and -0.5 percent error in the ROCs values of PR_2 and PR_3.

#96414 - $15.00 USD Received 19 May 2008; revised 17 Jun 2008; accepted 17 Jun 2008; published 23 Jun 2008

The SRC shows a similar behavior, any minor mismatch in the ROCs can be recovered by adjusting the telescope inside the SRC. However, these adjustments will change the Gouy phases inside both recycling cavities by up to 10°. This range has to be included in any follow-on analysis to calculate potential resonances of higher order modes inside the recycling cavities. Based on our results, the tolerances in the manufactured rOCs of these mirrors could be set by the available space to position the mirrors inside the vacuum chamber (typically on the order of 20 cm). This translates into a tolerance of 0.5% in ROC of PR_3 and SR_3. Much tighter tolerances have to be put on our knowledge of the ROCs before the mirrors can be installed or installation procedures have to be developed which allow to place the mirrors in the appropriate position for the as-build ROCs.

5.2. *Test masses*

The expected tolerances in the ROCs for the Advanced LIGO test masses are ± 10 m or about $\pm 0.5\%$ of the ~ 2000 m ROCs. These deviations from the nominal ROCs will change the eigenmode inside the arm cavities and will reduce the mode matching between the recycling cavities and the arm cavities. The left graph in Fig. 6 shows the mode matching between the eigenmode of the PRC and the eigenmode of the arm cavity as a function of the ROCs of the two test masses assuming that the recycling cavity mirrors are at their nominal position. Note that the ranges for the ROCs are already a factor of two larger than the above mentioned tolerances. Even without any corrections in the mode matching telescope, the mode matching will stay above 99.5%. This figure can also be used to estimate the mode mismatch between the two arm cavities. In the worst case, the mismatch will be twice what is shown in the graph when one set of mirrors is off by $+10$ m and the other by -10 m, respectively. The SRC shows a similar behavior.

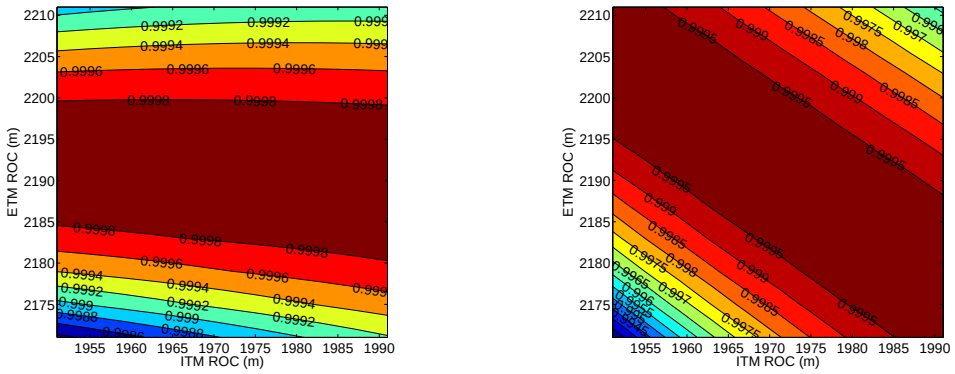

Fig. 6. The mode matching (in power) between the power recycling cavity and the (average) arm cavity as a function of ITM and ETM ROC. The left graph shows the mode matching w/o length adjustments. The mode matching between recycling cavity and arm cavity after adjusting the distances inside the beam expanding telescope becomes essentially 100.00%. The right graph shows the mode matching between the input mode cleaner and the power recycling cavity/arm cavity after adjusting the distances inside the power recycling cavity. These adjustments were made without changing the overall length of the recycling cavity and without changing the mode matching from the input mode. The mode matching between the output mode cleaner, the signal recycling cavity, and the arm cavities shows a similar behavior.

#96414 - $15.00 USD Received 19 May 2008; revised 17 Jun 2008; accepted 17 Jun 2008; published 23 Jun 2008

Adjusting the distance between PR_2 and PR_3 makes the mode matching between recycling cavity and arm cavity to virtually 100%. However, the mode matching from MC to the recycling cavity remains greater than 99.1% as shown in the right graph of Fig. 6. This assumes that the input mode is fixed. However, we can adjust the input mode by adjusting the mirrors present before PR_1 or by increasing the power from the laser. A 1% decrease can easily by adjusted by increasing the laser power without worrying about any additinal thermal effects. Similarly, for SRC, the output MC can be adjusted to the new SRC mode.

6. Summary

The PRC in the current LIGO detector consists essentially of flat mirrors and has a transversal mode spacing well below the linewidth of the cavity. Consequently, the spatial eigenmodes of the RF sidebands which are used to control all longitudinal and angular degrees of freedom are not well confined. Only the installation of a thermal correction system allowed LIGO to reach its current design sensitivity. The next major upgrade of LIGO, Advanced LIGO, will use power and signal recycling to enhance the carrier and the signal sidebands. In this paper we describe the new design for both recycling cavities which have well defined spatial eigenmodes and transversal mode spacings well above the linewidth of the cavities. We also discussed the allowed mode matching losses between the recycling cavities and the arm cavities. The main part of the paper shows that this new design is flexible enough and can be adjusted to easily accommodate ROC mismatches as long as the mismatches stay within some tolerances.

7. Appendix

A different concept for the stable recycling cavities with less optical components is often mentioned as an alternative to the three-mirror design presented in section 3. This concept uses only one focusing element in addition to the nominal recycling mirror. One version of this concept is shown in Fig. 7. A focusing lens (PR_2) which could be polished either into the substrate of the ITM or in the substrate of a compensation plate which will be located directly in front of the ITM. This lens would focus the beam over the length of the recycling cavity. The second element PR_1 would then be placed inside the Rayleigh range near the waist of the mode to accumulate a reasonable Gouy phase. An alternative design simply replaces the lens with a curved mirror similar to the curved mirror used in the three-mirror design.

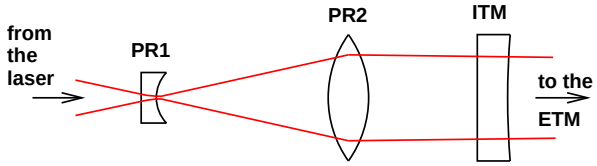

Fig. 7. A two element design for the stable recycling cavities. This design uses a focusing lens (PR2) and one curved mirror (PR1). The focusing lens could be formed inside the thermal compensation plate or inside the ITM substrate. Instead of a focusing lens, it is also possible to use a large curved mirror to focus the beam.

The main disadvantage of this design is that the divergence angle of the Gaussian mode would have to be:

$$\alpha = \frac{w_{ITM}}{L+\Delta} = \frac{w_0}{z_R} = \frac{\lambda}{\pi w_0}$$

where $w_{ITM} \approx 5.5\,\mathrm{cm}$ would be the beam size on PR_2, L is the distance to PR_1, $L+\Delta$ is the distance to the waist, w_0 is the waist of this mode, and z_R is the Rayleigh range. A distance L

#96414 - $15.00 USD Received 19 May 2008; revised 17 Jun 2008; accepted 17 Jun 2008; published 23 Jun 2008

that could fit into the LIGO vacuum envelope without folding the recycling cavity furthermore (which makes this a 3 mirror design) is $L \approx 25\,\mathrm{m}$. The distance between PR_1 and the waist of this mode Δ has to be in the order of the Rayleigh range to have any appreciable Gouy phase or transversal mode spacing inside the recycling cavity:

$$\Delta \approx z_R = \frac{\pi w_0^2}{\lambda} \qquad \Rightarrow \qquad \frac{w_{ITM}}{L + \frac{\pi w_0^2}{\lambda}} = \frac{\lambda}{\pi w_0}$$

Solving this for w_0 gives:

$$w_0 = \frac{w_{ITM}}{2} \pm \sqrt{\frac{w_{ITM}^2}{4} - \frac{L\lambda}{\pi}}$$

Using

$$\frac{L\lambda}{4} \approx 8.5 \times 10^{-6}\mathrm{m}^2 \ll 7.6 \times 10^{-4}\mathrm{m}^2 \approx \frac{w_{ITM}^2}{4}$$

we can expand the square root and use only the minus sign as the only reasonable physical solution:

$$w_0 = \frac{w_{ITM}}{2} - \frac{w_{ITM}}{2}\left(1 - \frac{\lambda L}{\pi}\frac{2}{w_{ITM}^2}\right) = \frac{\lambda L}{\pi w_{ITM}} \approx 154\,\mu\mathrm{m}$$

to calculate the waist of this mode. The beamsize on PR_1 would then be:

$$w_{PR1} = \sqrt{2} w_0 = 218\,\mu\mathrm{m}$$

The Rayleigh range of such a mode is:

$$z_R(\Delta = \pm z_R) = 7\,\mathrm{cm} \ll L$$

As this is much smaller than the distance between PR_2 and PR_1, the waist of this mode will also not change when we move it closer to PR_1 to change the Gouy phase. In general, any solution which generates a reasonable transversal mode spacing starting with a 5.5 cm and having only 25 m to work with will have to have a Rayleigh range of about 7 cm and beamsizes on PR_1 below $250\,\mu$m.

Small beamsizes such as this are usually associated with several potential problems. First of all, the intensity on PR_1 inside the power recycling cavity will reach a few $\mathrm{MW}/\mathrm{cm}^2$. This might cause life time problems with the coatings. Similar to the three mirror cavity, the short Rayleigh range makes this design very sensitive to ROC mismatches. This can also be compensated by changing the distance between PR_1 and PR_2. This length change would have to be compensated by also changing the distance between PR_2 and the ITM to maintain the overall length to keep the RF-sidebands resonant. Such a change is impossible when the focusing lens is polished into the ITM substrate and virtually impossible when it is polished into the compensation plate (CP) as the CP is suspended from the same suspension system than the ITM. The second design which uses the large curved mirror could accomodate this. However, this design requires to relay the laser beam to the other vacuum chamber and inject the beam from the other side which does not reduce the number of optical components in the entire setup, it tends to increase it.

Another problem of the small beamsizes is associated with alignment sensing and control. An angular motion of a cavity mirror will change the apparent length of the cavity if the beam is not centered on the rotation axis. This piston effect scales with the offset from the axis and the angle by which the mirror rotates. This is independent from the beamsize. But interferometric gravitational wave detectors use wavefront sensing to measure and suppress the angular motion.

#96414 - $15.00 USD Received 19 May 2008; revised 17 Jun 2008; accepted 17 Jun 2008; published 23 Jun 2008

These wavefront sensors measure the amplitude of the generated (1,0) and (0,1) Hermite Gauss mode. The amplitude scales with the beamsize on the rotated mirror:

$$a_{10} = \frac{\delta\alpha}{\lambda}\pi w.$$

Consequently, our sensing signals will be reduced proportional to the beamsize while the piston effect is independent from the beamsize. Larger beams make it easier to measure and control the rotation.

None of the above arguments completely rules out the use of a 2-mirror design for the recycling cavities, however, it does not appear to have any advantages over the three mirror design given the constrains of the current vacuum system and the current general layout.

Acknowledgments

The authors want to acknowledge the support of the LIGO Science Collaboration. Especially the discussions with Hiro Yamamoto, Peter Fritschel, Mike Smith, Bill Kells, Luke Williams, Garilynn Bilingsley, Dennis Coyne, Volker Quetschke, David Reitze, and David Tanner were very helpful. This work was supported by the National Science Foundation under grant PHY-0354999.

#96414 - $15.00 USD Received 19 May 2008; revised 17 Jun 2008; accepted 17 Jun 2008; published 23 Jun 2008